



ORIGINAL ARTICLE

Antiosteoporotic effects of *Alpinia officinarum* Hance through stimulation of osteoblasts associated with antioxidant effects



Yanjie Su ^{a,b,1}, Yahui Chen ^{a,1}, Yanzhi Liu ^a, Yajun Yang ^a,
Yifeng Deng ^a, Zhongqin Gong ^a, Jingfeng Chen ^a, Tie Wu ^a,
Sien Lin ^{b,c}, Liao Cui ^{a,*}

^a Department of Pharmacology, Guangdong Key Laboratory for Research and Development of Natural Drugs, Guangdong Medical University, Zhanjiang, China

^b Shenzhen Key Laboratory of R&D Laboratory of Space Medicine and Engineering Technology, Shenzhen Research Institute, The Chinese University of Hong Kong, Shenzhen, China

^c Department of Orthopaedics and Traumatology, The Chinese University of Hong Kong, Hong Kong, China

Received 30 April 2015; received in revised form 15 September 2015; accepted 28 September 2015
Available online 29 October 2015

KEYWORDS

Alpinia officinarum
Hance;
osteoblast;
osteoporosis;
ovariectomy;
oxidative stress

Summary *Background/Objective:* *Alpinia officinarum* Hance (AOH) is a traditional herbal medicine specific to south China and serves as a civil medication application of an antioxidant. Growing evidence demonstrates that antioxidants are beneficial for the treatment of osteoporosis. This study was designed to investigate the antiosteoporotic effects of total extracts from AOH in ovariectomised (OVX) rats and the different fractions in AOH on primary osteoblasts activities.

Methods: The total extract of AOH was extracted by refluxing using 95% ethanol, then the five fractions (F1–F5) were separated from AOH using thin-layer chromatography according to polarity from high to low, and the galangin content was determined using high performance liquid chromatography. In an *in vivo* study, 36 4-month-old female Sprague-Dawley rats were used as a Sham-operated group, OVX with vehicle (OVX), OVX with epimedium flavonoids (EF, 150 mg/kg/d), and OVX with AOH (AOH, 300 mg/kg/d), respectively. Daily oral administration started on Day 3 after OVX and lasted for 12 weeks. In the *in vitro* study, primary osteoblasts were incubated with AOH, galangin, and five different fractions (F1–F5) with or without hydrogen peroxide (H₂O₂), respectively.

* Corresponding author. No. 2, Wenming Donglu, Xiashan District, Zhanjiang, Guangdong Province, People's Republic of China.
E-mail address: cuiliao@163.com (L. Cui).

¹ These authors contributed equally to this work.

Results: Treatment with AOH significantly attenuated osteopenia accompanied by a decreased percentage of osteoclast perimeter and bone formation rate per unit of bone surface, enhanced the bone strength, and prevented the deterioration of trabecular microarchitecture associated with a decrease in biochemical parameters of oxidative stress. Furthermore, treatment with AOH, F3, F4, and galangin increased cell viability, differentiation, and mineralisation in osteoblasts with or without H₂O₂ and rescued the deleterious effects of H₂O₂ on cell apoptosis and intracellular reactive oxygen species level. The effects on osteoblast formation were highly aligned with the amounts of flavonoids within AOH.

Conclusion: These data demonstrate that ethanol extracts from AOH significantly reverse bone loss, partially by increasing bone formation, and by suppressing bone resorption associated with antioxidant effects, suggesting that AOH can be developed as a promising agent for the prevention and treatment of osteoporosis.

Copyright © 2015, The Authors. Published by Elsevier (Singapore) Pte Ltd. This is an open access article under the CC BY-NC-ND license (<http://creativecommons.org/licenses/by-nc-nd/4.0/>).

Introduction

Osteoporosis is a progressive systematic disease characterised by low bone mineral density (BMD) and deteriorated microarchitecture of bone which leads to an increase in the risk of fracture [1]. With the aging of the world's population, osteoporosis has become a serious global health problem. Several drugs are used to reduce bone loss in osteoporosis, including oestrogen, bisphosphonates, and parathyroid hormone, and many studies show that long-term use of these drugs might cause many adverse reactions, such as increasing the risk of endometrial and ovarian cancer [2,3], atypical femoral fractures [4], osteonecrosis of the jaw [5], venous thromboembolism [6], and nervous system disorders [7]. Consequently, it is necessary to develop an alternative with promising efficiency and fewer undesirable side effects to prevent or reverse postmenopausal osteoporosis.

Herbal medicine for the treatment of osteoporosis would be advantageous because they have potentially fewer side effects and multiple pharmacological actions on bone, making them more suitable for long-term use [8,9]. A number of medicinal herbs or natural compounds, such as epimedium [10], icariin [11], resveratrol [12], *Rhizoma drynariae* [13], and *Salvia miltiorrhiza bunge* [14], show preventive effects on bone loss induced by oestrogen deficiency, inflammation, or physical inactivity. They are cost-effective with few side effects and target multiple signalling pathways involved in bone metabolism [10–14]. *Alpinia officinarum* Hance (AOH) is a traditional herbal medicine within a strict growing area and specifically grows in south China. AOH is rich in bioactive phytochemical compounds such as flavonoids, diarylheptanoids, and essential oils, and it has been proven safe and is used for the treatment of a variety of diseases for a long time in China [15,16]. Many studies have shown that AOH presents anti-inflammatory and antioxidative properties both *in vitro* and *in vivo* [17–19]. AOH can exert an anti-amnesiac effect in A β -induced neurodegeneration in mice through an antioxidant property [19]. Flavonoids isolated from AOH mainly consist of quercetin, kaempferol, and galangin, which play a role in the protection against oxidative stress

by promoting the expression of antioxidative proteins [20]. Furthermore, quercetin can promote osteoblast differentiation and inhibit osteoclastogenesis via downregulation of mRNA expression of the *RANKL* gene in osteoblasts and subsequently inhibits osteoclastic function [21]. In addition, galangin, a flavonol derived from AOH, was proven to exert strong antioxidative and radical scavenging effects [22] and can reduce lipopolysaccharide-induced acute lung injury [23], fructose-induced rat liver injury [24], and fructose-induced rat kidney injury [25]. Moreover, galangin can prevent osteoclastic bone destruction and inhibit osteoclastogenesis via the attenuation of *RANKL*-induced c-Jun N-terminal kinases, p38, and nuclear factor-kappaB activation in osteoclast precursors as well as in collagen-induced arthritis mice [26].

A growing number of researches showed that oxidative stress is a pivotal reason for bone loss after the menopause and age-related bone loss [27,28]. Oxidative stress has been reported to inhibit osteoblastic differentiation and decrease the life span of osteoblasts, and also increase bone resorption by enhancing osteoclastic development and activity [29], thus, leading to a shift towards bone absorption more than bone formation, resulting in osteoporosis [30]. Antioxidant agents are beneficial for the treatment of osteoporosis by increasing bone formation or suppressing bone resorption [31,32]. Therefore, AOH with an antioxidative capacity may be developed as a novel agent for the prevention and treatment of osteoporosis. The present study was conducted to investigate the bone effects of AOH in ovariectomised (OVX) rats and to estimate different fraction compounds from AOH on the differentiation and antioxidative activities in primary osteoblasts *in vitro*.

Materials and methods

Preparation of total extract and five fractions (F1–F5) of AOH

The dried AOH was collected from Xuwen country, Guangdong, China. AOH (36 kg) was crushed into coarse power,

and then extracted six times with 98% ethanol. Afterwards, the leaching solution was collected and concentrated by evaporation to obtain the total extract of AOH to be used in the following steps. Then, AOH was further separated and purified with an ethyl acetate-petroleum ether (64:36) system, containing 2% acetic acid, and the extracts were separated into five fractions (F1–F5) according to the range from high to low polarity. The quality of the five fractions (F1–F5) was controlled by using thin layer chromatography and high performance liquid chromatography (HPLC). The chromatographic separation was achieved at 30°C on a Phenomenex C18 (Ø 250 mm × 4.6 mm, Agilent series 1100; Phenomenex Inc., Torrance, CA, USA) column. The run time was set at 40 minutes. The flow rate was 1.0 mL/min. The sample injection volume was 20 µL. The mobile phase was acetonitrile-0.2% H₃PO₄ solution (48:52). Galangin, as an ingredient of the extract, was purchased from the National Institutes for Food and Drug Control (Beijing, China).

Animals

Thirty-six 4-month-old virgin female Sprague–Dawley rats (obtained from the Centre of Experiment Animal of Sun Yat-sen University Ltd., Guangzhou, Guangdong, China) weighing 265 ± 14 g were used in this experiment [33]. All animals were acclimatised to local vivarium conditions (temperatures ranged from 24°C to 26°C, with a humidity level of 70%). During the experimental period, the rats were maintained on standard chow containing 1.33% calcium and 0.95% phosphate, and distilled water available *ad libitum*. The animals were treated in accordance with the Guide for Care and Use of Laboratory Animals by the National Committee of Science and Technology of China. The experimental protocol was approved by the institutional animal use and care review board of Guangdong Medical University, Zhanjiang, China.

Surgery and treatments

The acclimatised rats underwent either bilateral sham operation (SHAM, *n* = 8) or bilateral ovariectomy (OVX, *n* = 24, three groups with 8 rats/group) under general anaesthesia by 1% pentobarbital as previously described [34,35]. The OVX rats were then treated with a vehicle (OVX), epimedium flavonoids (EF, 150 mg/kg/d), or AOH (AOH, 300 mg/kg/d). EF was obtained from Xi'an Pulaite Biological Bioengineering Co., Xi'an, ShanXi, China. All treatments were performed by daily oral gavage from the 3rd day after surgery for 12 weeks. According to the Human Rat Equivalent Dose Conversion Principle [36,37] and the Chinese Pharmacopoeia, the experimental dose for AOH in the present study was equivalent to the corresponding clinical prescription dose for a 60-kg human participant. The experimental dose for epimedium flavonoids (150 mg/kg/d) in the present study was according to the previous study [38]. The body weight of rats was recorded weekly. All rats received a subcutaneous injection of calcein (10 mg/kg; Sigma Chemical Co., St. Louis, MO, USA) on Day 3, Day 4, Day 13, and Day 14 before sacrifice for *in vivo* double labelling.

At the endpoint, rats were anaesthetised with sodium pentobarbital (50 mg/kg intraperitoneally; Sigma Chemical

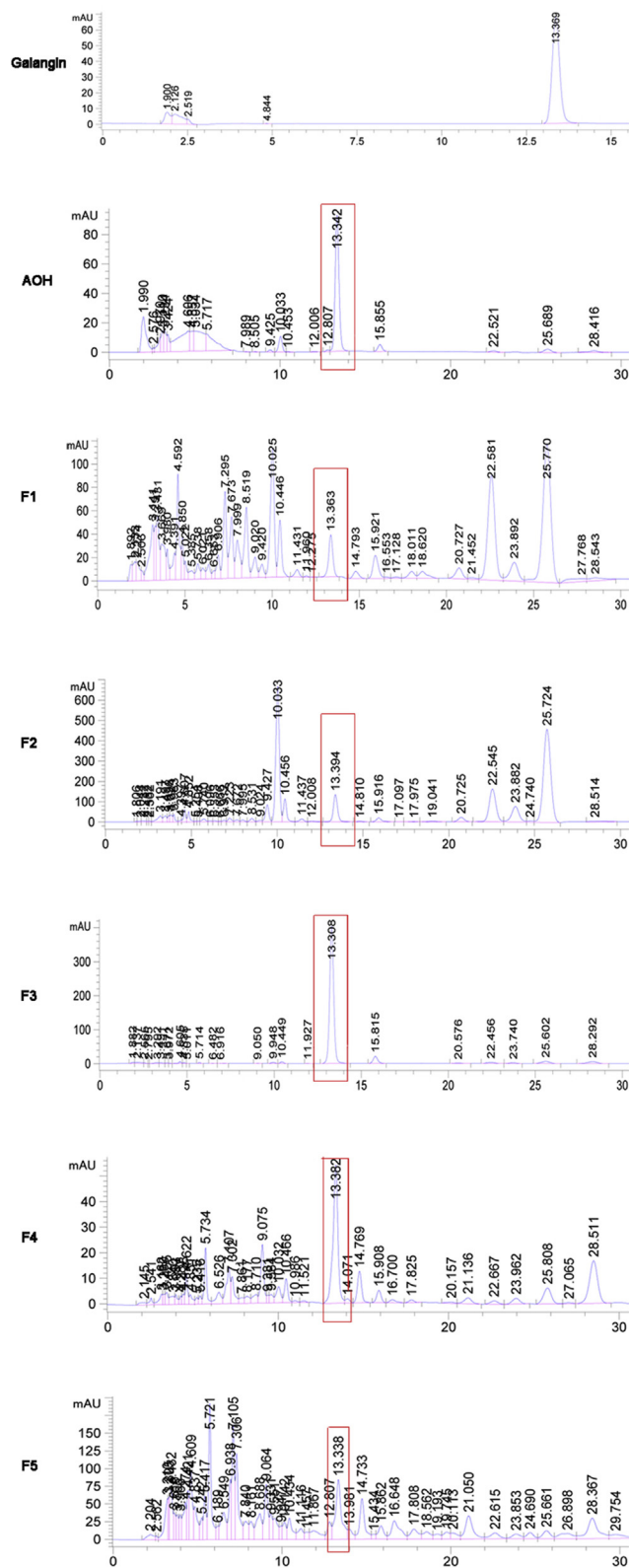


Figure 1 High performance liquid chromatography chromatograms of galangin, *Alpinia officinarum* Hance, and five fractions (F1–F5). X-axis is retention time (min). Y-axis is absorbance unit (mAU). AOH = *Alpinia officinarum* Hance.

Table 1 Content of galangin in *Alpinia officinarum* Hance and five fractions (F1–F5).

Fractions	AOH	F1	F2	F3	F4	F5
Percentage of galangin	0.519 ± 0.008	0.092 ± 0.004	0.384 ± 0.008	24.443 ± 0.087	0.191 ± 0.007	0.042 ± 0.003

Data are presented as mean ± standard deviation.

AOH = *Alpinia officinarum* Hance.

Co.) and euthanised. Blood and the right tibiae were collected for biochemical measurements. The uterus was collected and weighed. Left femurs and the fifth lumbar were dissected and stored at -20°C for measurement of bone mineral content (BMC) and BMD using dual-energy X-ray absorptiometry (DXA). Left femurs were collected for microcomputed tomography (μCT) analysis and followed by a three-point bending test. The left tibia was collected for bone histomorphometry. Right femurs were decalcified for histology and terminal deoxynucleotidyl transferase dUTP nick end labeling (TUNEL) assay.

Biochemical assays

Venous blood was collected and transferred to a centrifuge tube. Serum was prepared by centrifuging at 3000g for 10 minutes and stored at -80°C . The right tibia was washed to allow for bone marrow collection. Serum malondialdehyde (MDA), serum superoxide dismutase (SOD), and bone glutathione reductase (GSR) were measured using commercial kits and all procedures were performed according to the manufacturers' instruction (Nanjing Jiancheng Biological Bioengineering Co., Nanjing, China). An automatic plate reader (BioTek Instruments Inc., Winooski, VT, USA) was introduced to the measurements. Part of the bone marrow was centrifuged to obtain bone marrow cells. These cells were then labelled with 2',7'-dichlorofluorescein-diacetate (20M) for 30 minutes at 37°C and followed by measurement of fluorescence intensity using BD FACSCalibur flow cytometry (BD Biosciences, San Jose, CA, USA) [39]. Data were analysed and acquired using CellQuest Pro software (BD Biosciences).

DXA analysis

Two-dimensional BMC and BMD of the left femur and the fifth lumbar were measured using Lunar Prodigy Advance with a DXA scanner (GE Lunar Pharmalegacy Co., Fairfield, CT, USA) as previously described [40]. BMD was calculated by BMC of the measured area.

μCT analysis

Femurs were collected and performed in trabecular microarchitecture using a viva CT40 (Scanco Medical, Bruttisellen, Switzerland) in high resolution condition (X-ray energy 70KVp, 114Ma, 8W; integration time 200 msec; average data on 1) as reported elsewhere [41]. The femur was scanned from the distal growth plate to the proximal direction (18 $\mu\text{m}/\text{slice}$). To avoid primary spongiosa, the measurement site on the bone sections was the distal femur between 1 mm and 4 mm (160 slices) distal to the growth plate-epiphyseal junctions. Cortical bone analysis

was performed on a 1-mm region of interest from 7 mm (370 slices) distal to the growth plate-epiphyseal junctions. A threshold value of 200 was used to separate the trabecular bone from cortical bone in the analysis system in order to construct a three-dimensional image of the trabecular and cortical bone. After reconstruction, the following parameters were measured: relative bone volume to total volume (BV/TV), trabecula number (Tb.N), trabecula separation (Tb.Sp), trabecula thickness (Tb.Th), structure model index (SMI), connectivity density (Conn.D), cortical area (Ct.Ar), and cortical thickness (Ct.Th).

Bone histomorphometry

The left tibiae were removed and bone marrow cavities were exposed using a Low Speed Saw (Buehler Ltd., Chicago, IL, USA). The proximal tibial metaphyses were fixed in 10% buffered formalin for 24 hours followed by gradient

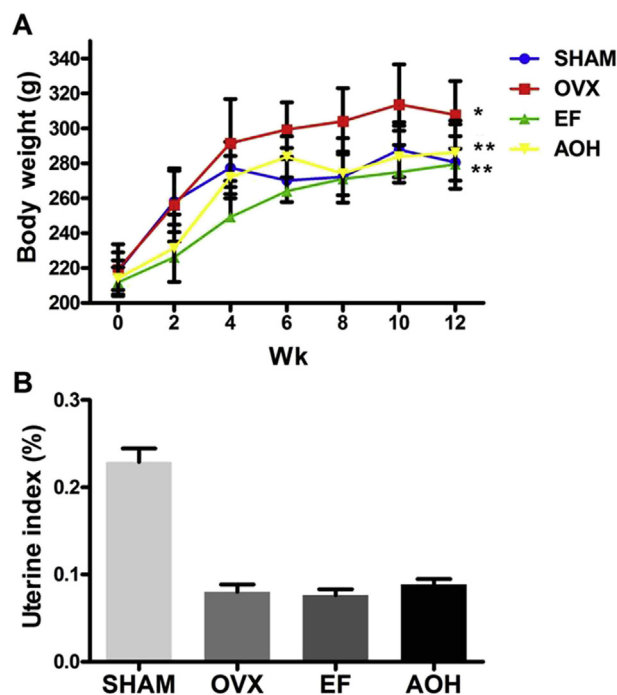


Figure 2 Effects of *Alpinia officinarum* Hance on (A) body weight and (B) uterus index in ovariectomised rats. Data are given as mean ± standard deviation. * $p < 0.05$ versus SHAM. ** $p < 0.05$ versus ovariectomised rats as evaluated by analysis of variance. SHAM = rats that underwent bilateral sham operation; OVX = rats that underwent bilateral ovariectomy and treated with vehicle; EF = rats that underwent bilateral ovariectomy and treated with epimedium flavonoids; AOH = rats that underwent bilateral ovariectomy and treated with *Alpinia officinarum* Hance.

Table 2 Effects of *Alpinia officinarum* Hance on biochemical markers of the blood and bone in ovariectomised rats.

Parameter	SHAM	OVX	EF	AOH
Serum SOD (U/mL)	94.61 ± 27.18	41.46 ± 5.97*	70.95 ± 23.96**	81.40 ± 6.77**
Serum MDA (µmol/L)	5.21 ± 2.08	15.64 ± 1.95*	9.59 ± 0.86**	5.89 ± 1.40**
Bone ROS (AFU × 1000)	1.17 ± 0.46	3.96 ± 0.78*	2.33 ± 0.52*,**	2.08 ± 0.27*,**
Bone GSR (mU/min/µg protein)	1.67 ± 0.31	0.30 ± 0.06*	1.08 ± 0.24*,**	0.81 ± 0.21*,**

Data are presented as mean ± standard deviation.

* $p < 0.05$ versus SHAM.

** $p < 0.05$ versus ovariectomised rats as evaluated by analysis of variance.

SHAM = rats that underwent bilateral sham operation; OVX = rats that underwent bilateral ovariectomy and treated with vehicle; EF = rats that underwent bilateral ovariectomy and treated with epimedii flavonoids; AOH = rats that underwent bilateral ovariectomy and treated with *Alpinia officinarum* Hance; SOD = superoxide dismutase; MDA = malondialdehyde; ROS = reactive oxygen species; GSR = glutathione reductase.

alcohol dehydration, defatted by xylene, and then embedded undecalcified in methyl methacrylate. The proximal tibial metaphysis was cut at a thickness of 9 µm and 5 µm with RM2155 hard tissue microtome (Leica AG, Wetzlar, Germany). The 9-µm unstained sections were used for dynamic histomorphometric analyses. The 5-µm sections were used for toluidine blue staining and Masson-Goldner Trichrome staining for the static histomorphometric measurements. A semiautomatic digitising image analysis system (Osteometrics, Atlanta, GA, USA) was used for quantitative bone histomorphometric measurements. The following parameters were measured: Tb.N, Tb.Sp, percent of osteoclasts perimeter (%Oc.Pm), bone formation rate per bone surface (BFR/BS), percent of the trabecular bone area (%Tb.Ar), percent of osteoblasts perimeter (%Ob.Pm), number of osteoclasts (Oc.N), and percent of labelled perimeter (%L.Pm).

Three-point bending test

Femurs were collected and bone biomechanical tests were performed on them using the 858 Mini Bionix material testing machine (MTS, Eden Prairie, MN, USA). Femurs were positioned horizontally with the anterior surface upwards and centred on the supports 10 mm apart. A displacement rate of 5 mm/min was selected for applying the loading vertically to the midshaft with anterior surface upward. Maximum load, breaking load, elastic load, and bending energy were obtained.

Histology and TUNEL assay

Light femurs were removed and bone marrow cavities were exposed using a Low Speed Saw (Buehler Ltd.), then fixed in 10% buffered formalin for 24 hours, followed by 75% alcohol, ethylenediaminetetraacetic acid-phosphate-buffered saline (PBS) solution, gradient alcohol dehydration, defatted by xylene, embedded in paraffin, cut at a thickness of 3 µm with RM2155 hard tissue microtome (Leica AG, Wetzlar, Germany), and then stained with haematoxylin-eosin, TUNEL, and 4',6-diamidino-2-phenylindole. The dyeing results were photographed using a fluorescence microscope. The number of fat cavitation and cell apoptosis were observed and compared.

Culture of rat osteoblasts

Rat osteoblasts (ROB) were isolated enzymatically from newborn rat calvariae as described in our previous literature [42]. Briefly, newborn rats were immersed in 75% alcohol for sterilisation, and then calvarias were isolated and cut into small pieces. Bone fragments were exposed to a solution containing trypsin for 15 minutes, followed by type I collagen enzyme for 1 hour. Cells were maintained in 25-cm² flasks in Dulbecco's modified Eagle's medium (Gibco, Carlsbad, CA, USA), supplemented with 100 U/mL penicillin, 100 µg/mL streptomycin, and 10% foetal bovine serum (Gibco) at 37°C in a humidified incubator with 5% CO₂. The medium was changed every 3 days.

Table 3 Effects of *Alpinia officinarum* Hance on bone mineral density and bone mineral content of femurs in ovariectomised rats.

Parameter	SHAM	OVX	EF	AOH
Femur BMD (g/mm ²)	0.28 ± 0.01	0.25 ± 0.02*	0.26 ± 0.01*	0.26 ± 0.08*,**
Femur BMC (g)	0.40 ± 0.02	0.37 ± 0.03*	0.37 ± 0.02*	0.38 ± 0.03
Lumbar BMD (g/mm ²)	0.27 ± 0.02	0.24 ± 0.01*	0.25 ± 0.01*	0.24 ± 0.02*
Lumbar BMC (g)	0.106 ± 0.011	0.09 ± 0.01*	0.09 ± 0.01*	0.09 ± 0.01*

Data are presented as mean ± standard deviation.

* $p < 0.05$ versus SHAM.

** $p < 0.05$ versus ovariectomised as evaluated by analysis of variance.

SHAM = rats that underwent bilateral sham operation; OVX = rats that underwent bilateral ovariectomy and treated with vehicle; EF = rats that underwent bilateral ovariectomy and treated with epimedii flavonoids; AOH = rats that underwent bilateral ovariectomy and treated with *Alpinia officinarum* Hance; BMD = bone mineral density; BMC = bone mineral content.

Cell viability

ROB were cultured in a 96-well plate at 6×10^3 cells/well and maintained in growth medium for 24 hours at 5% CO₂ at 37°C. After incubation with the different treatments above for 24 hours, 48 hours, or 72 hours, 10 µL of 3-(4,5-dimethylthiazol-2-yl)-2,5-diphenyltetrazolium bromide (MTT) medium (5 mg/mL) were added to each well. MTT mediums were replaced with 150 µL of solubilisation solution dimethyl sulfoxide after being cultured for an additional 4 hours, then vibrated slightly for 5 minutes. The value of optical density of each well was recorded at a wavelength of 570 nm using a microplate reader (Thermo Fisher Scientific, Vantaa, Finland).

Alkaline phosphatase activity

After 24 hours cultured in growth medium, ROB were treated with AOH, five fractions (F1–F5), or galangin with or without H₂O₂ in the osteogenic medium containing 10 µM β-glycerophosphate and 50 mg/mL ascorbic acid. Cells in 96-well plates cultured for 5 days, 7 days, or 9 days, were washed twice with 50 mM PBS (pH 7.4) and kept in 0.1% TritonX-100 lysis buffer overnight. Disodium 4-nitrophenyl phosphate buffer (6.7 mmol/L disodium p-nitrophenylphosphate hexahydrate, 25 mmol/L diethanolamine, and 1 mmol/L MgCl₂) was added in after cell thawing. NaOH was then added to terminate the reaction and the optical density was measured at a wavelength of 405 nm using a microplate reader (Thermo Fisher Scientific).

Alizarin red S stain

ROB were seeded in a 12-well plate and cultured for 24 hours, then treated with AOH, five fractions (F1–F5), or galangin with or without H₂O₂ in the osteogenic medium containing 10 µM β-glycerophosphate and 50 mg/mL ascorbic acid. The mediums were changed every 3 days. After 18 days, the cells were washed with PBS and fixed with 95% ice-cold alcohol for 15 minutes. The cells were then washed with PBS again, followed by 0.5% Alizarin Red S stain (pH = 4) for 30 minutes and subsequently washed three times with tap water. Pictures were taken using a Canon camera.

Analysis of apoptosis

Morphological alterations of apoptotic cells were observed using Hoechst 33258 staining. Briefly, cells were cultured at 1.5×10^5 cells/well in a 6-well plate. After being treated with AOH (10⁻⁵ g/mL), five fractions (F1–F5, 10⁻⁵ g/mL), and galangin (10⁻⁵ g/mL) with or without H₂O₂ (90 µM) for 24 hours, cells were washed with PBS and fixed with 4% paraformaldehyde for 10 minutes, followed by staining for 15 minutes with Hoechst 33258 (20 µM). Cells stained positive were photographed using a fluorescence microscope (Canon, Beijing, China).

Detection of intracellular reactive oxygen species level

To determine the level of reactive oxygen species (ROS) in H₂O₂-treated cells, osteoblastic cells were collected by trypsin digestion and resuspended in serum-free culture medium containing 10 µM 2',7'-dichlorofluorescein-diacetate for 30 minutes at 37°C. Subsequently, cells were washed with serum-free medium to remove free probes. The cells were then treated with vehicle control (control), H₂O₂ (100 µM), galangin (10⁻⁵ g/mL, positive control), F1 (10⁻⁵ g/mL), F3 (10⁻⁵ g/mL), or F4 (10⁻⁵ g/mL) for 30 minutes, followed by measurement of fluorescence intensity using BD FACSCalibur flow cytometry. Data were analysed and acquired using CellQuest Pro software (BD Biosciences).

Statistical analysis

Data were presented as mean ± standard deviation, and analysed using SPSS version 12.0 software for windows (SPSS Inc., Chicago, IL, USA). The statistical differences among groups were evaluated using variance with Fisher's protected least significant difference test. A *p* value < 0.05 was chosen to indicate significance.

Results

Compositional analysis of galangin from AOH and five fractions (F1–F5)

To determine the galangin content in each extract, AOH and five fractions were determined using HPLC and galangin served as a control sample. The HPLC fingerprint analysis of the extracts is shown in [Figure 1](#). The peak of galangin appeared when the retention time was 13.3 minutes. From the average peak areas of replicate injections, the content of galangin was calculated in AOH and the five fractions. As shown in [Table 1](#), AOH, F2, F3, and F4 contained more galangin than F1 and F5. AOH, F1, F2, F3, F4, and F5 contained galangin of 0.519%, 0.092%, 0.384%, 24.443%, 0.191%, and 0.042% respectively.

Body and uterine weights

As shown in [Figure 2](#), four groups of rats had a similar initial mean body weight. The body weight of the OVX group was significantly increased compared with the SHAM group (*p* < 0.05) on Week 4 after operation, and continued to be significantly higher throughout the study (*p* < 0.05). AOH and EF can significantly prevent the OVX-induced body weight gain at different scales from the beginning of the 2nd week (*p* < 0.05). OVX caused significant atrophy of uterine tissue compared with the SHAM group (*p* < 0.05), while AOH and EF did not elicit any uterotrophic effect.

Serum and bone biochemical markers of oxidative stress

As shown in [Table 2](#), compared with the SHAM group, serum SOD and bone GSR were significant decreased (*p* < 0.05),

Table 4 Effects of *Alpinia officinarum* Hance on bone parameters as measured by micro-computed tomography at the proximal femur in ovariectomised rats.

Parameter	SHAM	OVX	EF	AOH
Tb.N (1/mm)	5.28 ± 0.43	1.03 ± 0.18*	1.51 ± 0.33*	1.64 ± 0.27*,**
Tb.Th (mm)	0.12 ± 0.01	0.09 ± 0.01*	0.09 ± 0.01*	0.09 ± 0.01*
Tb.Sp (mm)	0.17 ± 0.02	1.06 ± 0.18*	0.74 ± 0.14*	0.67 ± 0.10*,**
BV/TV	0.44 ± 0.07	0.10 ± 0.03*	0.16 ± 0.04*	0.17 ± 0.02*,**
Conn.D (1/mm ³)	105.71 ± 15.68	28.05 ± 11.40*	39.77 ± 10.40*,**	45.51 ± 5.59*,**
SMI	-0.01 ± 0.65	2.02 ± 0.29*	1.74 ± 0.37*	1.72 ± 0.13*
Ct.Ar (mm ²)	6.84 ± 1.01	6.60 ± 1.12	5.96 ± 0.95	6.61 ± 0.96
Ct.Th (mm)	1.72 ± 0.13	1.66 ± 0.21	1.70 ± 0.10	1.70 ± 0.13

Data are presented as mean ± standard deviation.

**p* < 0.05 versus SHAM.

***p* < 0.05 versus ovariectomised rats as evaluated by analysis of variance.

SHAM = rats that underwent bilateral sham operation; OVX = rats that underwent bilateral ovariectomy and treated with vehicle; EF = rats that underwent bilateral ovariectomy and treated with epimedii flavonoids; AOH = rats that underwent bilateral ovariectomy and treated with *Alpinia officinarum* Hance; Tb.N = trabecula number; Tb.Th = trabecula thickness; Tb.Sp = trabecula separation; BV/TV = relative bone volume to total volume; Conn.D = connectivity density; SMI = structure model index; Ct.Ar = cortical area; Ct.Th = cortical thickness.

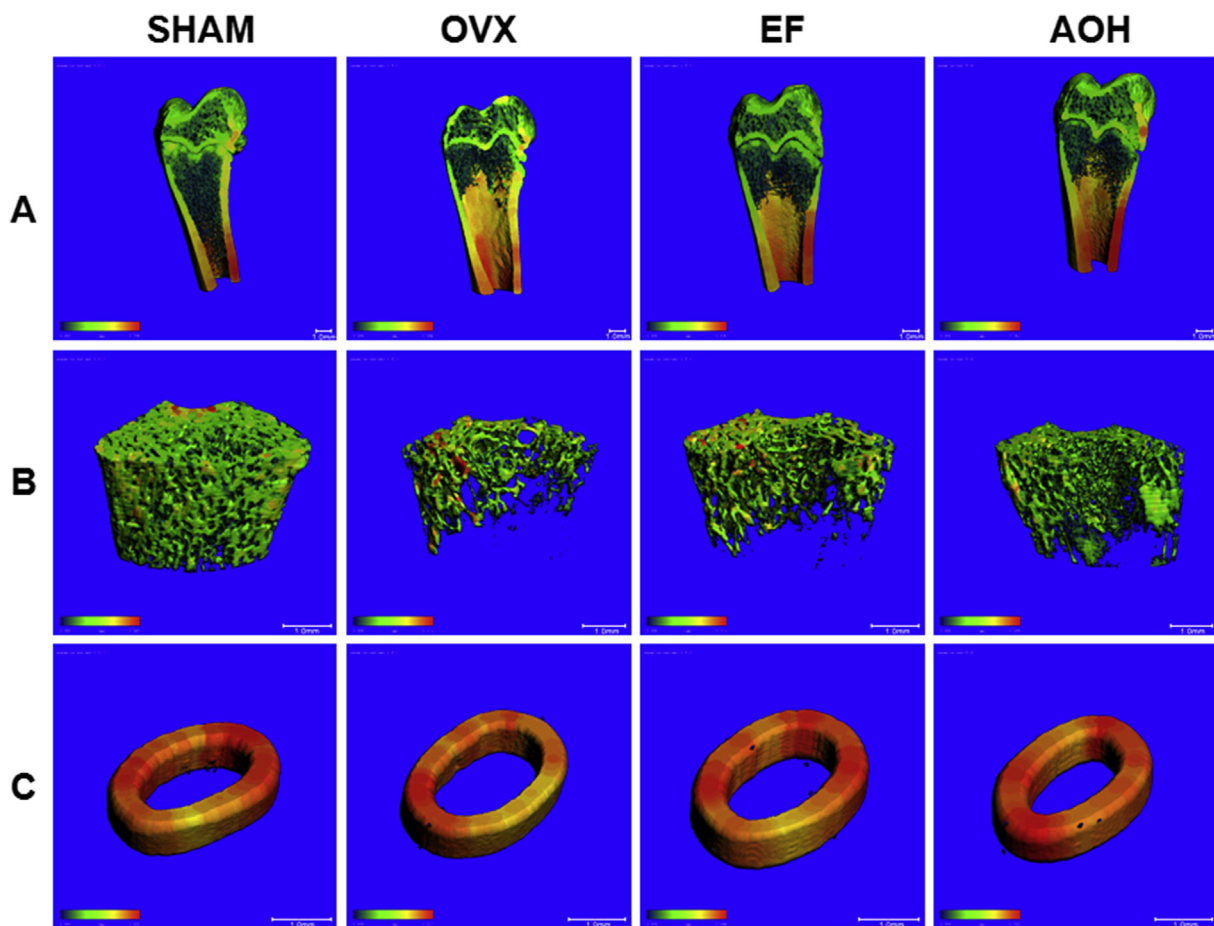


Figure 3 Micro-computed tomography (Viva CT40) scanning the architecture of trabecula bone and cortical bone within the distal metaphyseal region: (A) the whole bone; (B) the cancellous bone; (C) the cortical bone. SHAM = rats that underwent bilateral sham operation; OVX = rats that underwent bilateral ovariectomy and treated with vehicle; EF = rats that underwent bilateral ovariectomy and treated with epimedii flavonoids; AOH = rats that underwent bilateral ovariectomy and treated with *Alpinia officinarum* Hance.

Table 5 Effects of *Alpinia officinarum* Hance on proximal tibial metaphysis bone structure histomorphometry in ovariectomised rats (mean \pm standard deviation).

Parameter	SHAM	OVX	EF	AOH
Tb.Ar (%)	30.02 \pm 5.14	9.98 \pm 4.89*	12.42 \pm 3.10*	13.75 \pm 5.23*
Tb.N (#/mm)	5.81 \pm 0.79	2.11 \pm 0.95*	2.52 \pm 0.52*	2.98 \pm 1.07**
Tb.Sp (μ m)	123.20 \pm 24.89	526.25 \pm 267.01*	361.82 \pm 85.45*	317.19 \pm 92.26**
Ob.Pm (%)	0.84 \pm 0.14	1.98 \pm 0.64*	1.38 \pm 0.95	1.37 \pm 0.60
Oc.N (#/mm)	1.67 \pm 0.37	3.61 \pm 1.61*	2.54 \pm 0.55*	1.87 \pm 0.64**
Oc.Pm (%)	0.29 \pm 0.07	0.50 \pm 0.27*	0.56 \pm 0.14*	0.30 \pm 0.10**
L.Pm (%)	12.66 \pm 3.12	21.09 \pm 6.72*	18.40 \pm 8.82	16.43 \pm 4.77
BFR/BS (μ m/d \times 100)	8.69 \pm 2.18	20.78 \pm 8.23*	15.00 \pm 5.44	14.09 \pm 5.78**

Data are presented as mean \pm standard deviation.

* $p < 0.05$ versus SHAM.

** $p < 0.05$ versus ovariectomised rats as evaluated by analysis of variance.

SHAM = rats that underwent bilateral sham operation; OVX = rats that underwent bilateral ovariectomy and treated with vehicle; EF = rats that underwent bilateral ovariectomy and treated with epimedium flavonoids; AOH = rats that underwent bilateral ovariectomy and treated with *Alpinia officinarum* Hance; Tb.Ar = trabecular bone area; Tb.N = trabecula number; # = number; Tb.Sp = trabecula separation; Ob.Pm = osteoblasts perimeter; Oc.N = number of osteoclasts; Oc.Pm = osteoclasts perimeter; L.Pm = labelled perimeter; BFR/BS = bone formation rate per bone surface.

whereas serum MDA and bone ROS increased ($p < 0.05$) in the OVX group. Compared with the OVX group, serum SOD and bone GSR were significantly increased ($p < 0.05$), while serum MDA and bone ROS were significantly decreased ($p < 0.05$) in the AOH group and the EF group.

BMD

As shown in Table 3, compared with the SHAM group, a significant reduction in BMD of the femur by 10.7% ($p < 0.05$) and lumbar by 8.9% ($p < 0.05$) was observed in the OVX group. Compared with the OVX group, the rats

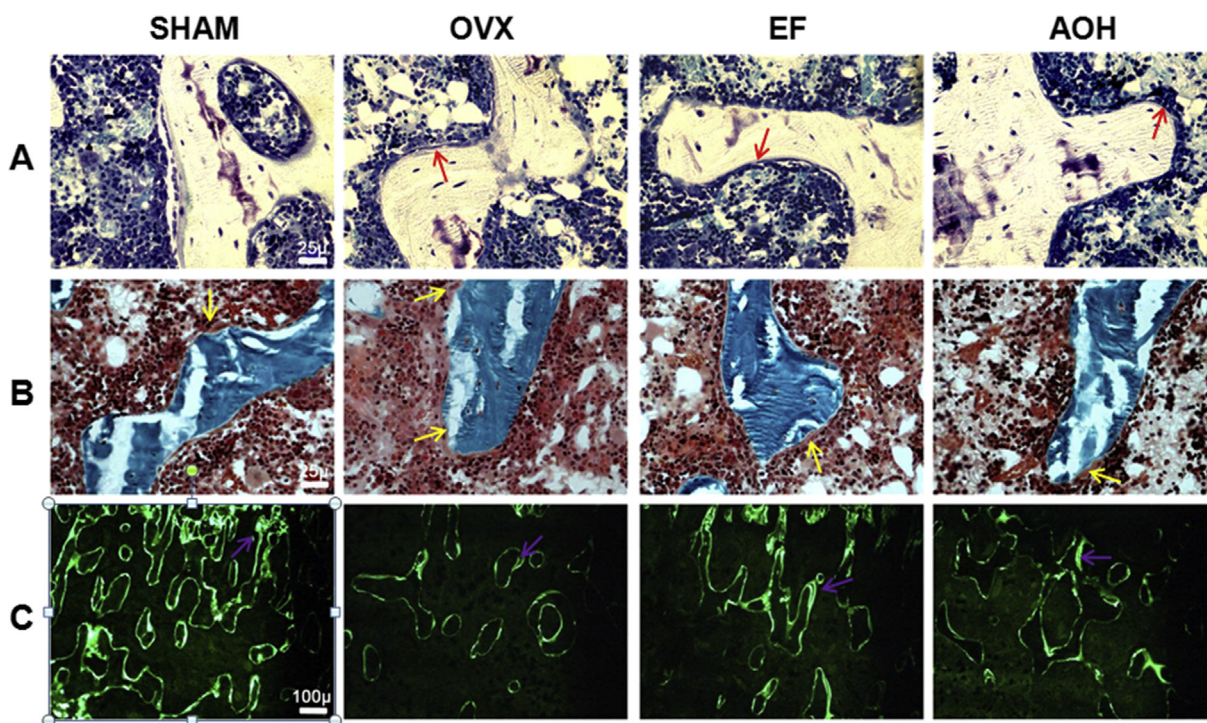


Figure 4 Effects of *Alpinia officinarum* Hance (AOH) on osteoblasts, osteoclasts, and fluorescence in the proximal tibial metaphysis in ovariectomised rats: (A) toluidine blue staining ($\times 400$, osteoblasts: red arrows); (B) Masson–Goldner trichrome staining ($\times 400$, osteoclasts: yellow arrows); (C) fluorescence ($\times 100$, double fluorescence: purple arrows). Osteoblasts and osteoclasts were active in the OVX group, whereas most of the osteoblasts and osteoclasts were inactive in the AOH and EF groups. Double fluorescence labelling was obvious in the OVX group, while it was dimming in the AOH and EF groups. SHAM = rats that underwent bilateral sham operation; OVX = rats that underwent bilateral ovariectomy and treated with vehicle; EF = rats that underwent bilateral ovariectomy and treated with epimedium flavonoids; AOH = rats that underwent bilateral ovariectomy and treated with *Alpinia officinarum* Hance.

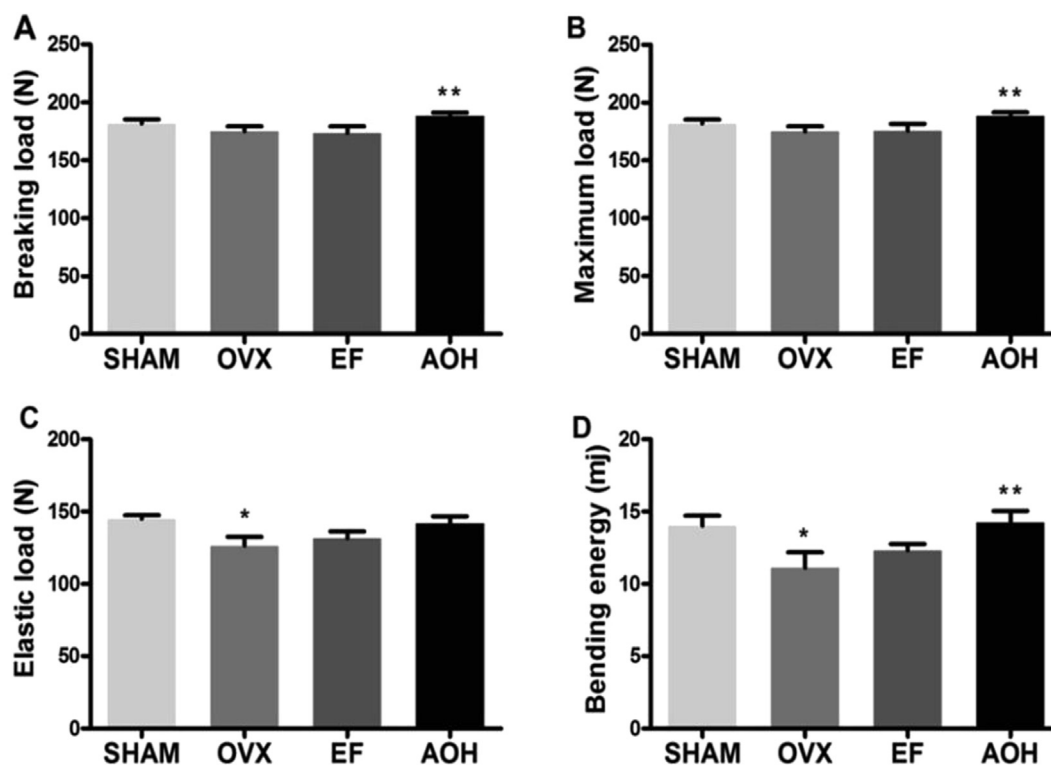


Figure 5 Effects of *Alpinia officinarum* Hance on bone biomechanical properties in femurs in ovariectomised rats. Values are mean \pm standard error of the mean. * $p < 0.05$, versus SHAM. ** $p < 0.05$ versus ovariectomised rats as evaluated by analysis of variance.

SHAM = rats that underwent bilateral sham operation; OVX = rats that underwent bilateral ovariectomy and treated with vehicle; EF = rats that underwent bilateral ovariectomy and treated with epimedium flavonoids; AOH = rats that underwent bilateral ovariectomy and treated with *Alpinia officinarum* Hance.

treated with AOH showed a significant increase in BMD of the femur by 4.8% ($p < 0.05$), while the BMD of the lumbar showed no significant change. The rats treated with EF also showed no significant change in the femur and lumbar compared with the OVX group. Compared with the SHAM

group, a significant reduction ($p < 0.05$) in BMC of the femur by 10.2% ($p < 0.05$) and lumbar by 11.4% ($p < 0.05$) was observed in the OVX rats. However, there were no differences in femur and lumbar BMC in all treatment groups.

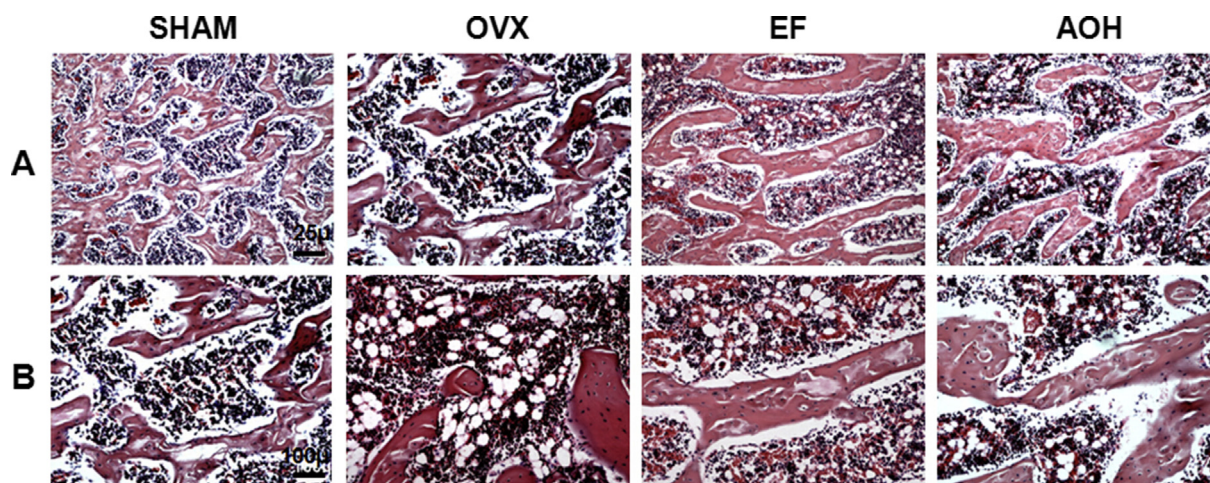


Figure 6 Effects of *Alpinia officinarum* Hance (AOH) on the number of the fat cavitation in the proximal femoral metaphysis in ovariectomised rats: (A) $\times 40$; and (B) $\times 100$. SHAM = rats that underwent bilateral sham operation; OVX = rats that underwent bilateral ovariectomy and treated with vehicle; EF = rats that underwent bilateral ovariectomy and treated with epimedium flavonoids; AOH = rats that underwent bilateral ovariectomy and treated with *Alpinia officinarum* Hance.

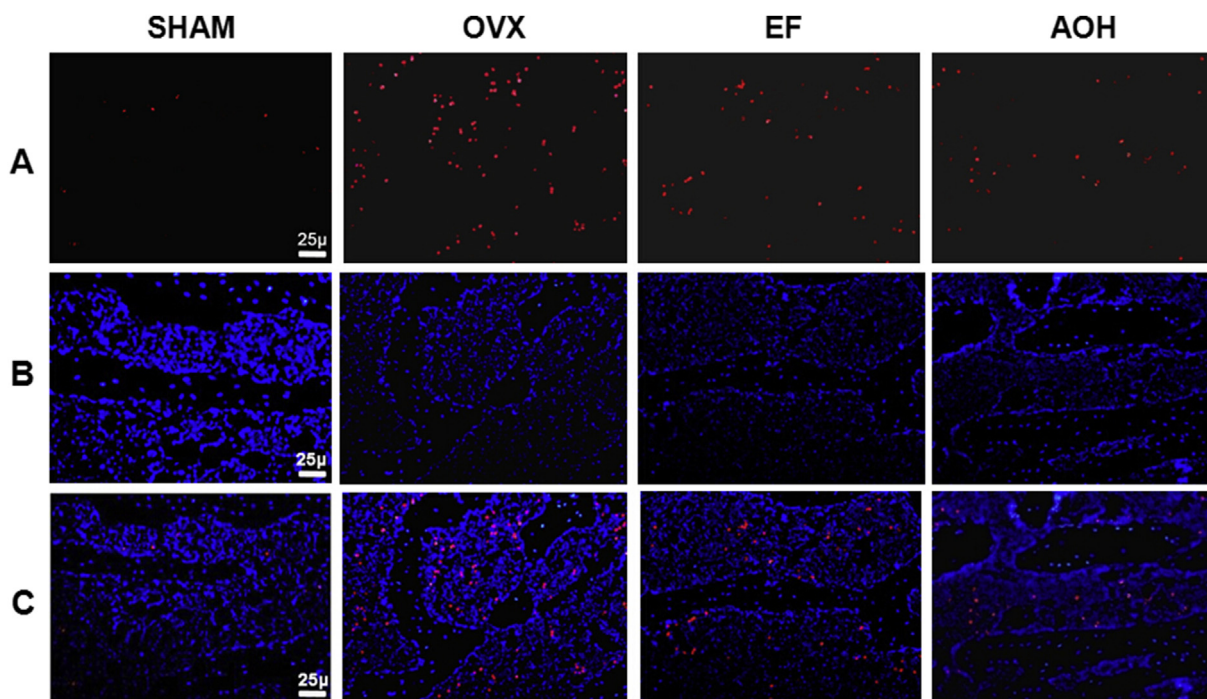


Figure 7 Effects of *Alpinia officinarum* Hance (AOH) on cell apoptosis in the proximal femoral metaphysis in ovariectomised rats: (A) terminal deoxynucleotidyl transferase dUTP nick end labeling staining ($\times 40$); (B) 4',6-diamidino-2-phenylindole staining ($\times 40$); (C) A and B merged. The number of cell apoptosis events was increased in the ovariectomised group. SHAM = rats that underwent bilateral sham operation; OVX = rats that underwent bilateral ovariectomy and treated with vehicle; EF = rats that underwent bilateral ovariectomy and treated with epimedii flavonoids; AOH = rats that underwent bilateral ovariectomy and treated with *Alpinia officinarum* Hance.

Bone microarchitecture

As shown in Table 4 and Figure 3, three-dimensional images of femoral metaphysis showed significant difference in trabecular microarchitecture between the SHAM and OVX groups. Briefly, compared with the SHAM group, BV/TV, Tb.N, and Tb.Th were significantly decreased by 76.0% ($p < 0.05$), 80.5% ($p < 0.05$), and 21.0% ($p < 0.05$), respectively, while Tb.Sp, Conn.D, and SMI in the proximal femur were significantly increased by 73.5% ($p < 0.05$) and 12,930.0% ($p < 0.05$) in the OVX group. Compared with the OVX group, BV/TV, Tb.N, and Conn.D were significantly increased by 59.6% ($p < 0.05$), 59.6% ($p < 0.05$), and 62.2% ($p < 0.05$) in the AOH group ($p < 0.05$), respectively, while Tb.Sp was significantly decreased by 36.3% in the AOH group ($p < 0.05$), and SMI showed no significant change in the AOH group ($p > 0.05$). Compared with the OVX group, BV/TV, Tb.N, Tb.Th, SMI, and Tb.Sp showed no significant change, while Conn.D was significantly increased by 53.4% in the EF group ($p < 0.05$). Furthermore, there were no significant changes in Ct.Ar and Ct.Th among all groups.

Bone histomorphometry

Static and dynamic histomorphometric measurements of the proximal tibia are illustrated in Table 5 and Figure 4. When compared with the SHAM group, Tb.N and %Tb.Ar were significantly decreased by 63.7% ($p < 0.05$) and 66.7% ($p < 0.05$), while Tb.Sp, %Ob.Pm, %Oc.Pm, Oc.N, BFR/BS,

and %L.Pm were significant increased, respectively, by 327.2% ($p < 0.05$), 136.5% ($p < 0.05$), 71.1% ($p < 0.05$), 116.5% ($p < 0.05$), 138.9% ($p < 0.05$), and 66.6% ($p < 0.05$) in the OVX group. Compared with the OVX group, Tb.N was

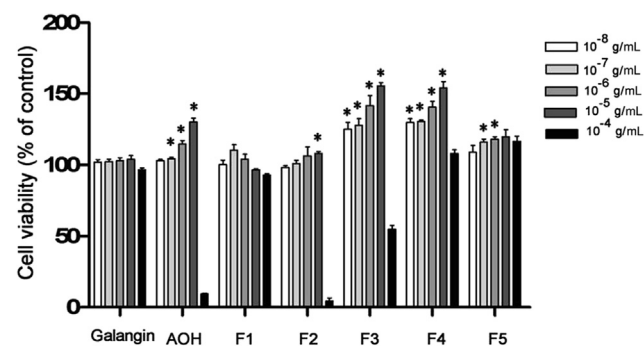


Figure 8 Effects of five fractions (F1–F5) isolated from *Alpinia officinarum* Hance on the viability of primary rat osteoblasts. Osteoblasts were treated with concentrations ranging from 10^{-8} g/mL to 10^{-4} g/mL of galangin, *Alpinia officinarum* Hance, or the five fractions (F1–F5) for 24 hours. Cell viability was measured by 3-(4,5)-dimethylthiazoliazolium bromide (3-(4,5)-dimethylthiazolium bromide) (-z-y1)-3,5-di-phenyltetra zolium bromide (MTT) assay. Data are given as mean \pm standard deviation of at least three independent experiments. Data are expressed as a percentage of control. * $p < 0.05$ versus control. AOH = *Alpinia officinarum* Hance.

significantly increased by 41.1% ($p < 0.05$), while Tb.Sp, Oc.N, %Oc.Pm, and BFR/BS were significantly increased by 39.7% ($p < 0.05$), 48.3% ($p < 0.05$), 39.7% ($p < 0.05$), and 32.2% ($p < 0.05$) in the AOH group, respectively. Compared with the OVX group, static and dynamic histomorphometric measurements of the proximal tibia had no significant change in the EF group.

Bone biomechanical properties

As shown in Figure 5, compared with the SHAM rats, elastic load and bending energy were significantly decreased by 12.9% ($p < 0.05$) and 20.7% ($p < 0.05$), respectively, and maximum load and breaking load showed no significant decrease ($p > 0.05$) in OVX group rats. Compared with the OVX rats, the rats treated with AOH significantly increased ($p < 0.05$) in maximum load, breaking load, and bending energy by 7.8% ($p < 0.05$), 7.6% ($p < 0.05$), and 27.9% ($p < 0.05$), respectively, but with no significant increase ($p > 0.05$) in elastic load. No significant difference was found between the OVX and EF groups.

Cells apoptosis and fat cavitation of bone marrow

As shown in Figures 6 and 7, compared with the SHAM group, there were more numbers of fat cavitation and cell apoptosis in the OVX group in the proximal femoral metaphysis. Whereas compared with the OVX group, the number of fat cavitation and cell apoptosis events were decreased in the AOH and EF groups.

Effects of five fractions (F1–F5) isolated from AOH on osteoblast viability

As shown in Figure 8, an increase in viability was observed in cells treated with AOH at the concentration of 10^{-7} g/mL to 10^{-5} g/mL. Osteoblasts treated with F3 and F4 at a concentration from 10^{-8} g/mL to 10^{-5} g/mL showed a distinct trend towards elevation in a concentration-dependent manner, while at concentrations up to 10^{-4} g/mL showing an inhibitory effect on cell proliferation. However, osteoblasts treated with F1, F2, and F5 showed no significant alterations at all concentrations indicated. In particular, galangin as a positive control showed no effect on cell viability at 24 hours, while cell viability showed a distinct trend towards an increase in a time-dependent manner at different time points from 24 hours, 48 hours, to 72 hours in cells treated with 10^{-5} g/mL galangin (data not shown).

Effects of five fractions (F1–F5) isolated from AOH on osteoblast alkaline phosphatase activity

As shown in Figure 9, alkaline phosphatase (ALP) activity in primary osteoblasts exposed to galangin, AOH, F3, and F4 at concentrations of 10^{-8} g/mL to 10^{-5} g/mL remarkable increased, while ALP activities in F1, F2, and F5 groups have no alterations during the experimental period indicated above. Interestingly, the effects of galangin reached the climax of ALP activity at 7 days for an approximate 150%

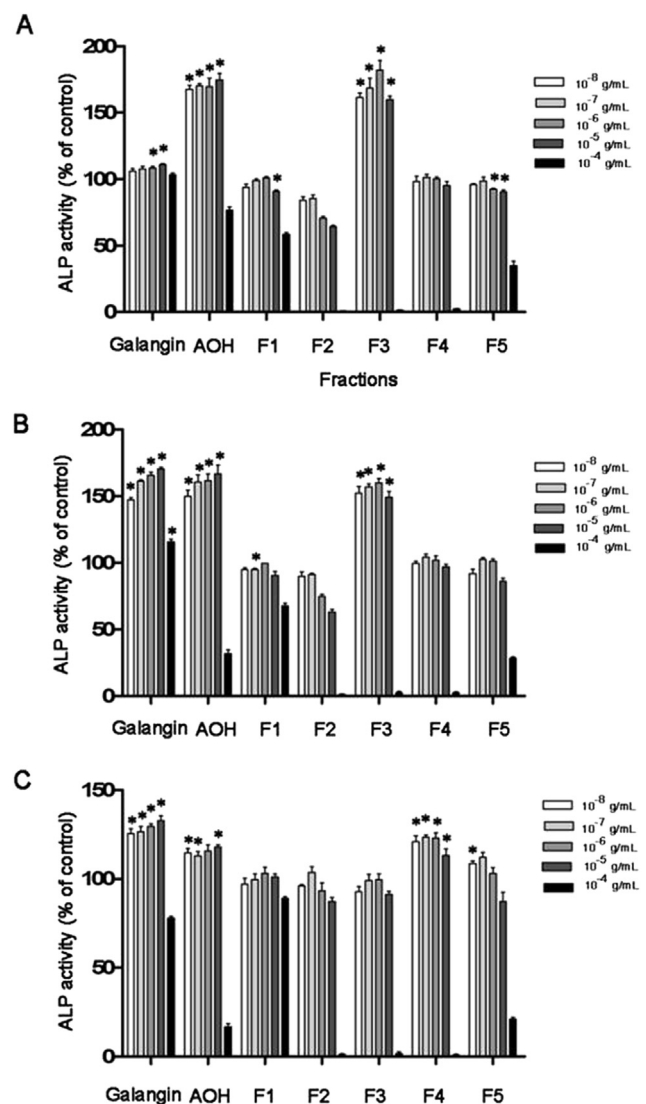


Figure 9 Effects of five fractions (F1–F5) isolated from *Alpinia officinarum* Hance on the differentiation of primary rat osteoblasts. Alkaline phosphatase activity (measured by optical density value) was determined after exposure to galangin, *Alpinia officinarum* Hance, or five fractions (F1–F5) for a period of 5 days (A), 7 days (B), and 9 days (C). ALP = alkaline phosphatase; AOH = *Alpinia officinarum* Hance.

higher than vehicle control and lasted 9 days, while the effect of AOH and F3 on ALP activities were driven over 150% higher than the vehicle control at 5 days and trended towards a reduction at 9 days. Moreover, the effect of F4 exhibited no change at 5 days, but exhibited an extraordinary trend increase at 9 days and reached a peak approximately 125% higher than the vehicle control.

Effects of five fractions (F1–F5) isolated from AOH on osteoblast calcification

Mineralised capacity in primary osteoblasts stimulated with AOH and five fractions (F1–F5) was detected with Alizarin Red S staining assay after 18 days. As shown in Figure 10,

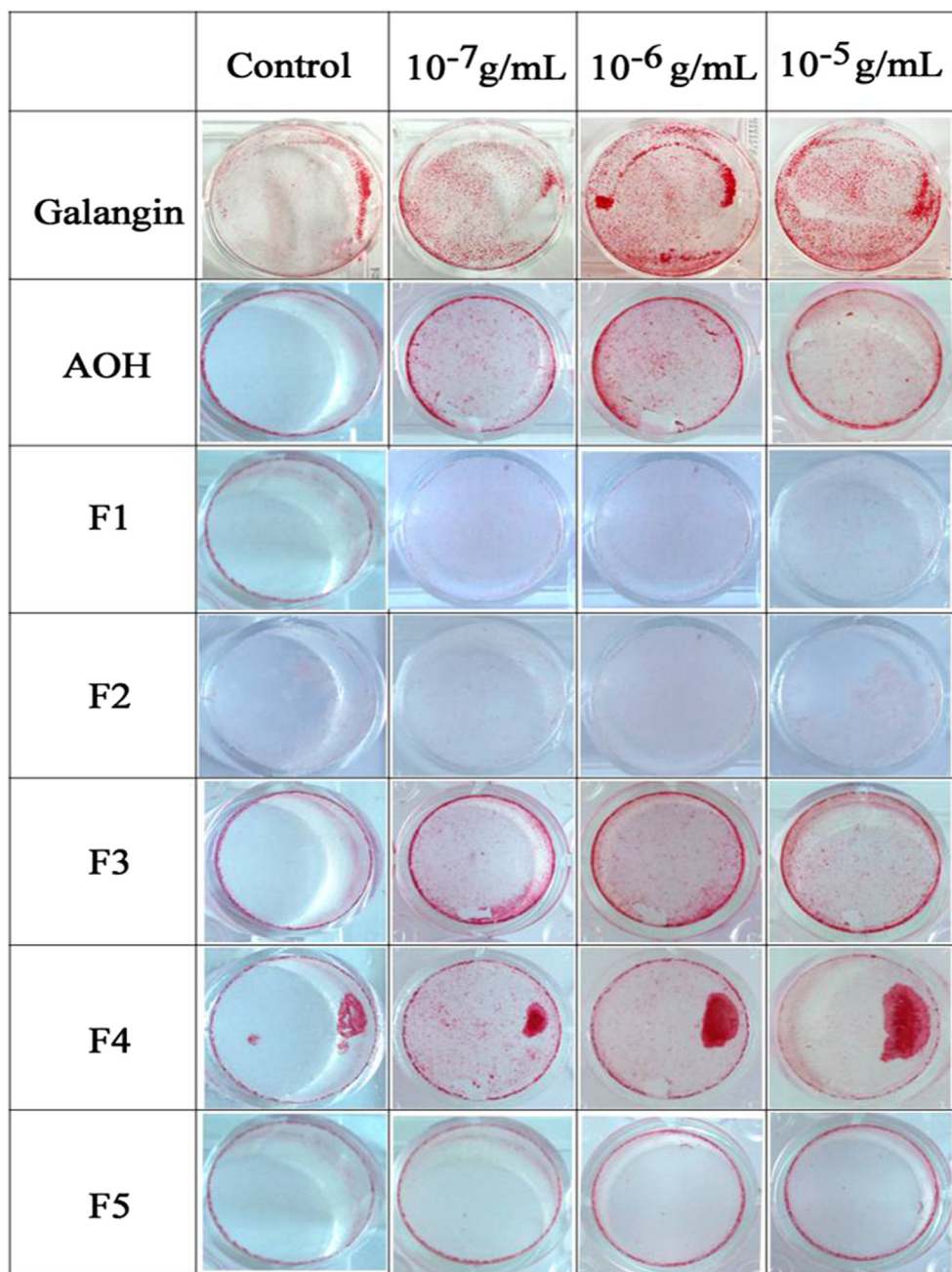


Figure 10 Dose-dependent effects of galangin, *Alpinia officinarum* Hance, and five fractions (F1–F5) on rat osteoblasts mineralisation. Cells were cultured in osteogenic medium containing 10 mM L-glycerophosphate and 50 μ g/mL ascorbic acid in the presence or absence of indicated drugs. Mineralisation activity was stained using alizarin red S after 18 days of treatment. AOH = *Alpinia officinarum* Hance.

galangin, AOH, F3, and F4 markedly promoted mineralised nodules formation at the concentration of 10^{-7} g/mL to 10^{-5} g/mL when compared with the control. Meanwhile, no stimulated effects were observed in osteoblastic cells treated with F1, F2, and F5 compared with the control.

Collectively, according to the evidence of cell viability, ALP activity assay, and osteoblast calcification, AOH, F3, and F4 were selected for further study in subsequent experiments.

Effects of F3 and F4 isolated from AOH on primary osteoblasts viability treated with oxidative stress

To elucidate the proper concentration of H_2O_2 on cell viability, MTT assay was used in primary osteoblasts viability. Osteoblast cells were treated with H_2O_2 ranging from 10 μ M to 100 μ M for a period of 24 hours. As shown in [Figure 11A](#), the lower concentration (≤ 60 μ M) showed no effect on cell growth, while the higher concentration

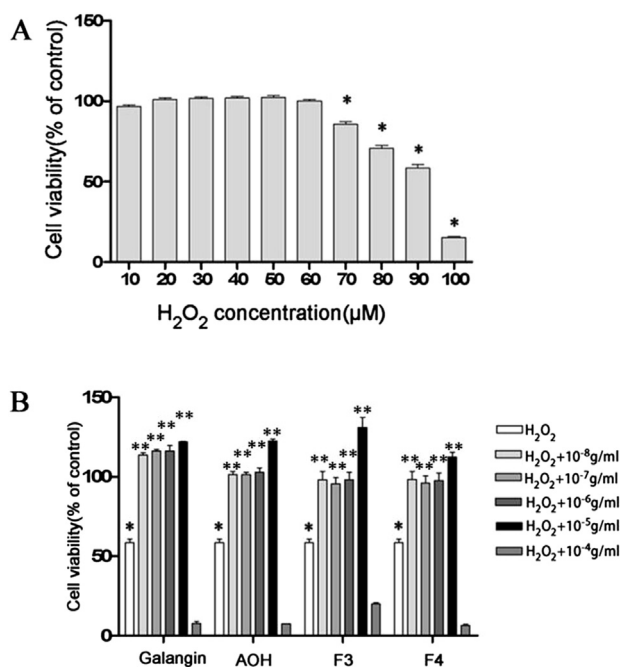


Figure 11 Protective effects of galangin, *Alpinia officinarum* Hance, F3, and F4 against H₂O₂-induced cell injury in rat osteoblasts. (A) Cell viability was measured by 3-(4,5-dimethyl-2-thiazolyl)-2,5-diphenyl-2-H-tetrazolium bromide (MTT) assay in osteoblasts exposed to H₂O₂ at the indicated concentration for 24 hours. (B) Osteoblasts were pretreated in the presence or absence of *Alpinia officinarum* Hance, F3, F4, or galangin for 1 hour before the addition of H₂O₂ (90 μM) and were cultured for 24 hours. AOH = *Alpinia officinarum* Hance.

(≥70 μM) showed an apparent trend in inhibitory action. Being treated with 90 μM H₂O₂ exhibited an approximate one half decrease, therefore, H₂O₂ at the concentration of 90 μM was used for following experiment.

To further investigate the protective effects of AOH, F3, and F4 on rat osteoblasts against H₂O₂ damage, we cultured cells in the presence of 90 μM H₂O₂ with or without treatment of AOH, F3, F4, or galangin at the concentration of

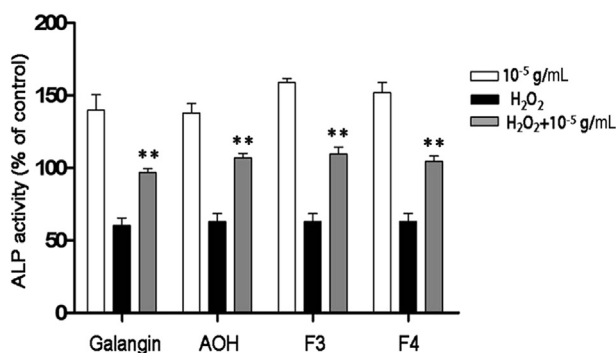


Figure 12 *Alpinia officinarum* Hance, F3, F4, or galangin compete H₂O₂ induced cell injury on osteoblastic differentiation. Cells were pretreated with or without *Alpinia officinarum* Hance, F3, F4, or galangin before the addition of H₂O₂ (90 μM). Alkaline phosphatase activity was detected at Day 7. *p < 0.05 versus control. **p < 0.05 versus H₂O₂ (90 μM). ALP = alkaline phosphatase; AOH = *Alpinia officinarum* Hance.

10⁻⁸ g/mL to 10⁻⁴ g/mL. As shown in Figure 11B, treatment with H₂O₂ (90 μM) contributed to suppression of cell viability, which could be hindered markedly by AOH, F3, F4, or galangin (10⁻⁸ g/mL to 10⁻⁵ g/mL) in a dose-dependent manner, reaching a climax high at a concentration of 10⁻⁵ g/mL. Based on the previous evidence, AOH, F3, and F4 with a concentration of 10⁻⁵ g/mL were adopted to further study in the subsequent measurements.

Effects of F3 and F4 isolated from AOH on cell ALP activity treated with oxidative stress

Primary osteoblasts exposed to H₂O₂ were cocultured with galangin, AOH, F3, and F4 for 5 days, 7 days, and 9 days for detecting alterations of ALP activity. As shown in Figure 12, H₂O₂ (90 μM) was found to have an inhibitory effect on ALP activity in rat osteoblasts, which was reversed by treatment with 10⁻⁵ g/mL of AOH, F3, or F4, as effectively as galangin.

Effects of F3 and F4 isolated from AOH on osteoblast nodule formation treated with oxidative stress

As shown in Figure 13, the extent of Alizarin Red S staining declined dramatically in primary osteoblasts exposed to H₂O₂, while the antagonistic effect of H₂O₂ on mineralisation was markedly rescued by AOH, F3, or F4, and especially by AOH group.

Effects of F3 and F4 isolated from AOH on ROS production induced by oxidative stress

As shown in Figure 14, the results showed that incubation with 90 μM H₂O₂ markedly increased intracellular ROS levels, and addition of AOH, F3, and F4 at a concentration of 10⁻⁵ g/mL significantly attenuated ROS production. Compared with the control group, H₂O₂ (90 μM) showed an increase in ROS level by 20%. Compared to the H₂O₂ group, galangin, AOH, F3, and F4 demonstrated a decrease in ROS level by 15%, 22.3%, 16.7%, and 3.3%, respectively. These results revealed that AOH, F3, and F4 abated H₂O₂-induced oxidative stress by scavenging ROS generation in osteoblasts.

Effects of F3 and F4 isolated from AOH on ROB apoptosis by oxidative stress

As shown in Figure 15, apoptotic cells characterised by chromatin condensation, apoptotic bodies, and nuclear fragments were observed in ROB treated with H₂O₂ (90 μM). Coincubation with AOH, F3, or F4 in osteoblastic cells can significant reduce the apoptotic extent elicited by H₂O₂.

Discussion

Our study, for the first time, has demonstrated the beneficial effects of AOH against osteopenia in OVX rats and five fractions of AOH containing different content of flavonoids (i.e., galangin) on the differentiation and antioxidative

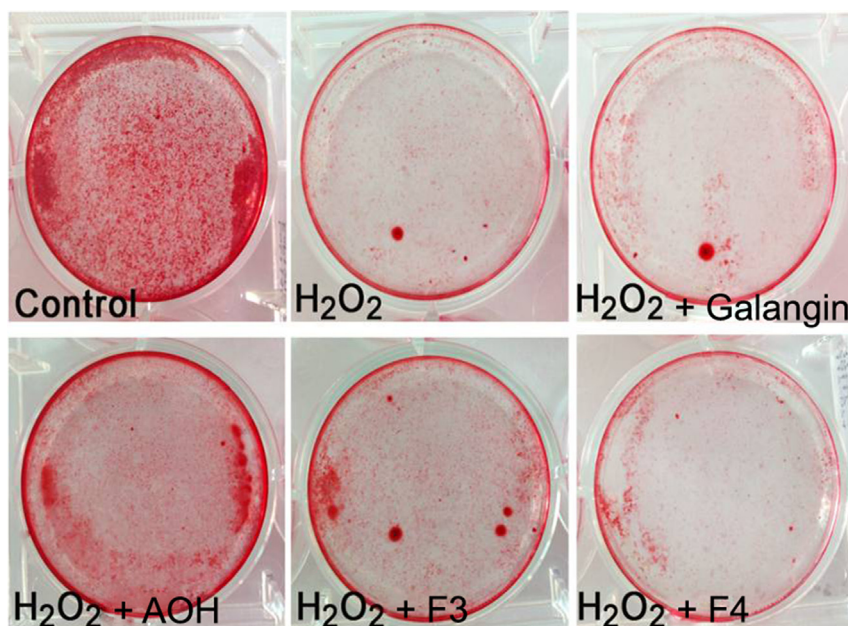


Figure 13 *Alpinia officinarum* Hance, F3, F4, or galangin attenuate H_2O_2 induced cell mineral formation injury on osteoblastic mineralisation. AOH = *Alpinia officinarum* Hance.

activities in osteoblasts *in vitro*. The major findings of the present study are as follows: (1) treatment with total extract of AOH partially prevented bone loss, significantly improved bone microarchitecture, bone strength, and oxidative stress status in OVX-induced osteoporotic rats; (2)

in addition, AOH exerted a better effect on osteopenia related to the decrease of osteoclast surface and bone turnover rate in OVX rats than that of epimedium flavonoids; (3) AOH, F3, F4, and galangin can rescue the deleterious impacts of oxidative stress on osteoblastic

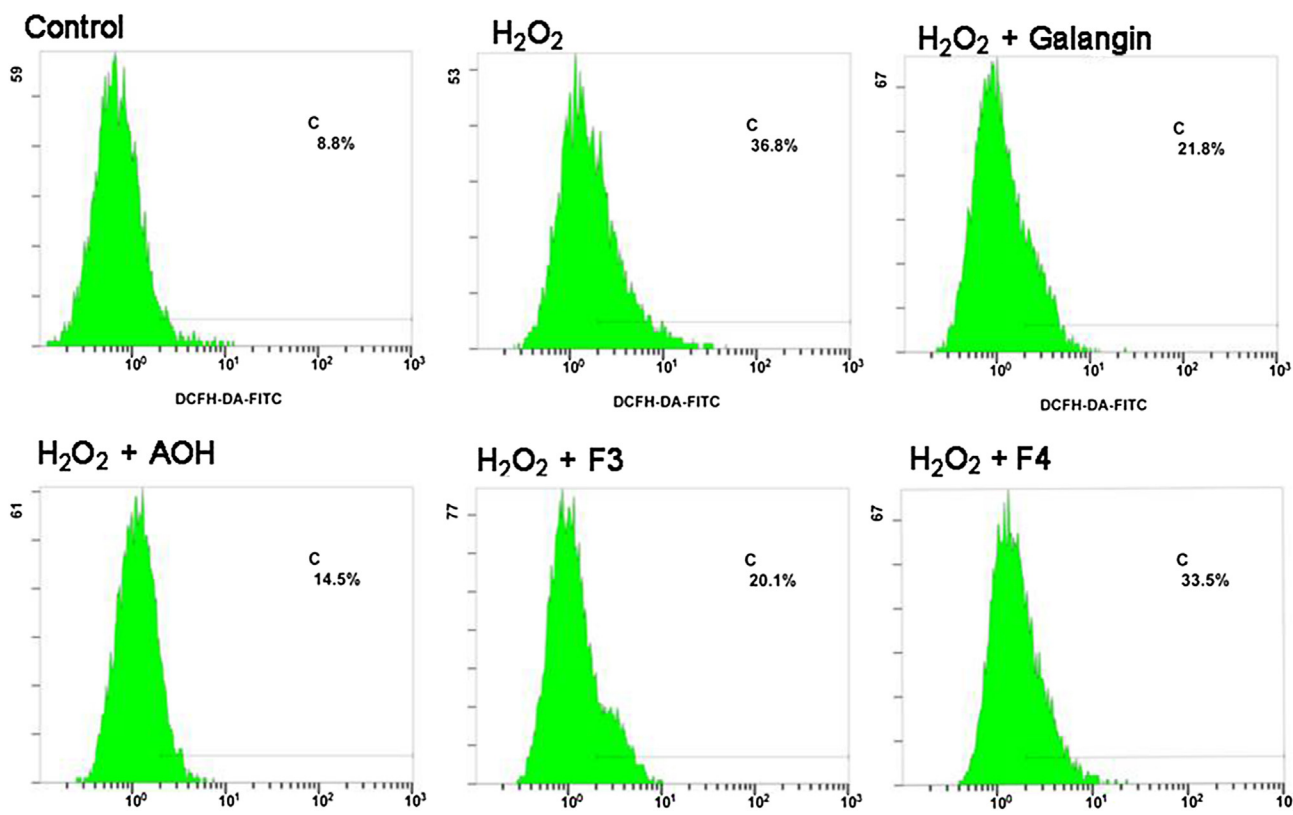


Figure 14 Coincubation with *Alpinia officinarum* Hance, F3, F4, or galangin and H_2O_2 (90 μ M) reduces reactive oxygen species production after induction of oxidative stress. AOH = *Alpinia officinarum* Hance; DCFH-DA-FITC = dichloro-dihydro-fluorescein diacetate-fluorescein isothiocyanate.

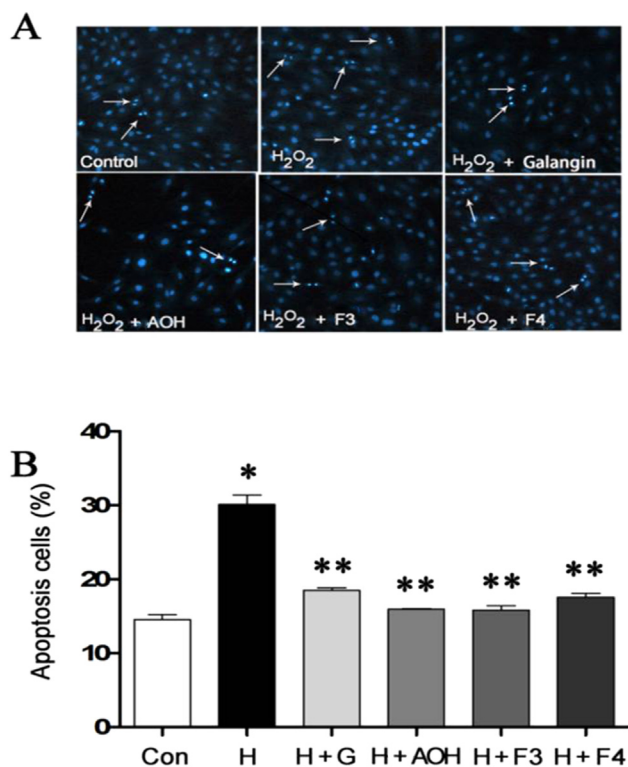


Figure 15 *Alpinia officinarum* Hance, F3, F4, or galangin counteract inhibitory effect on H_2O_2 -induced cell apoptosis in rat osteoblasts. Cell apoptosis was detected by Hoechst 33258 staining in cells treated with Con, H, H + G, H + *Alpinia officinarum* Hance, H + F3, and H + F4 for 24 hours. Arrows identify cells with condensed or fragmented nuclei, characteristic of apoptosis. * $p < 0.05$ versus control. ** $p < 0.05$ versus H_2O_2 (90 μ M). Con = vehicle control; H = H_2O_2 (90 μ M); H + G = H_2O_2 (90 μ M) + galangin (10⁻⁵ g/mL); H + AOH = H_2O_2 (90 μ M) + *Alpinia officinarum* Hance (10⁻⁵ g/mL); H + F3 = H_2O_2 (90 μ M) + F3 (10⁻⁵ g/mL); H + F4 = H_2O_2 (90 μ M) + F4 (10⁻⁵ g/mL).

differentiation; however, F1, F2, and F5 have no effect on promoting osteoblastic differentiation. It is indicated that the protective effect in OVX rats and in osteoblast differentiation *in vitro* could be partly related to higher galangin content within AOH. Taken together, these results suggest that AOH can be developed as a potential and promising agent for the prevention and treatment of osteoporosis.

In this study, we found that AOH has an excellent value in reversing bone loss of the femur evidenced by a significant increase in BMD, BV/TV, and Tb.Th, and a decrease in Tb.Sp, indicating that AOH could increase bone mass. Furthermore, bone histomorphometry results demonstrated that treatment with AOH could partially prevent osteopenia and decrease bone turnover induced by ovariectomy. AOH significantly increased %Tb.Th, while clearly decreased Tb.Sp, %Oc.Pm, Oc.N, and BFR/BS of the tibia. Performing a three-point bending tests on femoral diaphysis, we found that AOH prevented bending energy decreases in OVX rats and increased maximum and fracture force, indicating that AOH could improve bone biomechanical properties. Many studies have found that

flavonoids isolated from AOH consist mainly of quercetin, kaempferol, and galangin which can promote osteoblasts differentiation and inhibit osteoclastogenesis via down-regulation of mRNA expression of the *RANKL* gene in osteoblasts and subsequently inhibit osteoclastic function [21,26]. Those effects of AOH were similar to that of EF, which additional studies have confirmed. However, as a reference compound, the reported dose of EF cannot show an achievement effect over AOH. Moreover, AOH significantly decreased the number of fat cavitation and cell apoptosis in the proximal femoral metaphysis in OVX rats and showed better effects than EF. Taken together, these results suggest that the antiosteoporosis effects of AOH relate not only to flavonoids, but also to diarylheptane and volatile oil.

To further explore the underlying mechanisms of the protection effect of AOH and to understand the biochemistry relative to the effect of AOH, five fractions (F1–F5) were isolated from AOH and treatment of their capacity of osteoblast differentiation and mineralisation. The data demonstrated that five fractions (F1–F5) and AOH with the concentration ranging from 10⁻⁴ g/mL to 10⁻⁸ g/mL for 24 hours, 48 hours, and 72 hours showed no cytotoxicity in rat osteoblastic cells. However, AOH, F3, and F4 stimulated osteoblastic proliferation, differentiation, and mineralisation. By contrast, osteoblasts treated with F1, F2, and F5 exhibited no actions on osteoblastic development compared with the vehicle control. The studies indicated that AOH, F3, and F4 could be the most potent compositions in the present study, protecting osteoblasts against cell apoptosis induced by OVX. As shown in our results, F3 and F4 both contain higher amounts of galangin than F1 and F5. Therefore, we speculate that the effect of different fractions of AOH on osteoblastic differentiation could be highly related to the effects of galangin. AOH works better than F3, while it contains lower amounts of galangin than F3, it is likely to have other substances that play a role. Further research is required to address and expand the present findings.

Another finding is that AOH could suppress the increase in the weight of the OVX rats and cannot restore the atrophic uterus. It suggests that AOH may prevent bone loss by other mechanisms rather than influencing oestrogen levels. At present, oxidative stress has been considered increasingly as an important risk factor of age-associated diseases including osteoporosis [43]. Generally, excessive ROS accumulation cannot be efficiently scavenged by an antioxidant defence system, contributing to oxidative stress and subsequently to bone loss [44]. Epidemiological evidence has demonstrated that antioxidants exert a protective effect on the development of osteoporosis [45]. Based on well-documented evidence highlighting the role of oxidative stress in osteoporosis, we investigated firstly that the fractions extracted from AOH showed a strong antioxidant effect responsible for the protection of osteoblastic differentiation. Therefore, we investigated the protective effects of AOH to OVX-induced oxidative damage in rats and the different fractions (F1–F5) from AOH on H_2O_2 -induced oxidative damage in primary osteoblasts. In an *in vivo* study, there were significant reductions in SOD and GSR levels, improvement in bone marrow cell apoptosis and pimplis, but increments in MDA and ROS levels of

ovariectomised rats compared with baseline rats. These results are consistent with a previous study [46] which found that OVX rats had a clear reduction in SOD enzyme. Although treatment with AOH significantly reduced SOD and GSR levels, and improved the bone marrow cell apoptosis and pimeiosis, it increased MDA and ROS levels of ovariectomised rats. In an *in vivo* study, we found that H₂O₂ could provoke the increase of ROS generation and subsequently results in a decrease in cell viability, differentiation, mineralisation, and apoptosis, which is consistent with previous studies [47,48]. AOH, F3, and F4 counteracted the inhibitory effect of H₂O₂-induced oxidative stress on osteoblasts apoptosis, differentiation, mineralisation, and ROS generation. These results strongly support the viewpoint that AOH could scavenge ROS and subsequently attenuate oxidative stress *in vitro* and *in vivo*.

AOH is extensively used in food flavouring and as an anti-inflammatory agent for musculoskeletal diseases, including rheumatism, in Chinese and Ayurvedic medicine for >2500 years [49,50]. Relevant clinical research results found that AOH extract had a statistically significant effect on reducing symptoms of osteoarthritis of the knee with a good safety profile and just mild gastrointestinal adverse events [51]. All these pieces of evidence prove the safety of the clinical application of AOH.

In summary, the present study demonstrates that AOH significantly partially reversed ovariectomised bone loss by increasing bone formation and suppressing bone resorption associated with antioxidant effects, which suggests that AOH can be developed as a promising agent for the prevention and treatment of osteoporosis. Further studies are desirable to explore the active ingredients, mechanisms of AOH on osteoclasts and other animal models of osteoporosis, the pharmaceutical preparation, and the toxicity of its preparation, to provide preclinical evidence for the prevention of osteoporosis for its clinical application in the future.

Conflicts of interest

All authors state that they have nothing to disclose and declare no conflicts of interest.

Funding/support

This study was supported by grants-in-aid from the National Natural Science Foundation of China (No. 81273518) and the Science and Technology Planning Project of Guangdong Province (2012B060300027).

References

- [1] Gass M, Dawson-Hughes B. Preventing osteoporosis-related fractures: an overview. *Am J Med* 2006;119:S3–11.
- [2] Strom BL, Schinnar R, Weber AL, Bunin G, Berlin JA, Baumgarten M, et al. Case-control study of postmenopausal hormone replacement therapy and endometrial cancer. *Am J Epidemiol* 2006;164:775–86.
- [3] Danforth KN, Tworoger SS, Hecht JL, Rosner BA, Colditz GA, Hankinson SE. A prospective study of postmenopausal hormone use and ovarian cancer risk. *Br J Cancer* 2007;96:151–6.
- [4] Park-Wyllie LY, Mamdani MM, Juurlink DN, Hawker GA, Gunraj N, Austin PC, et al. Bisphosphonate use and the risk of subtrochanteric or femoral shaft fractures in older women. *JAMA* 2011;305:783–9.
- [5] Marx RE. Pamidronate (Aredia) and zoledronate (Zometa) induced avascular necrosis of the jaws: a growing epidemic. *J Oral Maxillofac Surg* 2003;61:1115–7.
- [6] Clemett D, Spencer CM. Raloxifene: a review of its use in postmenopausal osteoporosis. *Drugs* 2006;60:379–411.
- [7] Rizzoli R, Reginster JY, Boonen S, Bréart G, Diez-Perez A, Felsenberg D, et al. Adverse reactions and drug-drug interactions in the management of women with postmenopausal osteoporosis. *Calcif Tissue Int* 2011;89:91–104.
- [8] Leung PC, Siu WS. Herbal treatment for osteoporosis: a current review. *J Tradit Complment Med* 2013;3:82–7.
- [9] Mukwaya E, Xu F, Wong MS, Zhang Y. Chinese herbal medicine for bone health. *Pharm Biol* 2014;52:1223–8.
- [10] Xu YX, Wu CL, Wu Y, Jin HT, Yu NZ, Xiao LW. Epimedium-derived flavonoids modulate the balance between osteogenic differentiation and adipogenic differentiation in bone marrow stromal cells of ovariectomised rats via Wnt/ β -catenin signal pathway activation. *Chin J Integr Med* 2012;18:909–17.
- [11] Feng R, Feng L, Yuan Z, Wang D, Wang F, Tan B, et al. Icaritin protects against glucocorticoid-induced osteoporosis *in vitro* and prevents glucocorticoid-induced osteocyte apoptosis *in vivo*. *Cell Biochem Biophys* 2013;67:189–97.
- [12] Durbin SM, Jackson JR, Ryan MJ, Gigliotti JC, Alway SE, Tou JC. Resveratrol supplementation preserves long bone mass, microstructure, and strength in hindlimb-suspended old male rats. *J Bone Min Metab* 2014;32:38–47.
- [13] Guo D, Wang J, Wang X, Luo H, Zhang H, Cao D, et al. Double directional adjusting estrogenic effect of naringin from *Rhizoma drynariae* (Gusuibu). *J Ethnopharmacol* 2011;138:451–7.
- [14] Cui L, Li T, Liu Y, Zhou L, Li P, Xu B, et al. Salvianolic acid B prevents bone loss in prednisone-treated rats through stimulation of osteogenesis and bone marrow angiogenesis. *PLoS One* 2012;7:e34647.
- [15] Bu X, Xiao G, Gu L. Chemical study of *Alpinia officinarum*. *Zhong Yao Cai* 2000;23:84–7.
- [16] Lee J, Kim KA, Jeong S, Lee S, Park HJ, Kim NJ, et al. Anti-inflammatory, anti-nociceptive, and anti-psychiatric effects by the rhizomes of *Alpinia officinarum* on complete Freund's adjuvant-induced arthritis in rats. *J Ethnopharmacol* 2009;126:258–64.
- [17] Srividya AR, Dhanabal SP, Misra VK, Suja G. Antioxidant and antimicrobial activity of *Alpinia officinarum*. *Indian J Pharm Sci* 2010;72:145–8.
- [18] Chang CL, Lin CS, Lai GH. Phytochemical characteristics, free radical scavenging activities, and neuroprotection of five medicinal plant extracts. *Evid Based Complement Altern Med* 2012;2012. Article ID 984295, 8 pages.
- [19] Hanish Singh JC, Alagarsamy V, Sathesh Kumar S, Narsimha Reddy Y. Neurotransmitter metabolic enzymes and antioxidant status on Alzheimer's disease induced mice treated with *Alpinia galanga* (L.) Willd. *Phytother Res* 2011;25:1061–7.
- [20] Hanneken A, Lin FF, Johnson J, Maher P. Flavonoids protect human retinal pigment epithelial cells from oxidative-stress-induced death. *Invest Ophthalmol Vis Sci* 2006;47:3164–77.
- [21] Satue M, Arriero Mdel M, Monjo M, Ramis JM. Quercitrin and taxifolin stimulate osteoblast differentiation in MC3T3-E1 cells and inhibit osteoclastogenesis in RAW 264.7 cells. *Biochem Pharmacol* 2013;86:1476–86.
- [22] Zhang W, Lan Y, Huang Q, Hua Z. Galangin induces B16F10 melanoma cell apoptosis via mitochondrial pathway and sustained activation of p38 MAPK. *Cytotechnology* 2013;65:447–55.

- [23] Shu YS, Tao W, Miao QB, Lu SC, Zhu YB. Galangin dampens mice lipopolysaccharide-induced acute lung injury. *Inflammation* 2014;37:1661–8.
- [24] Sivakumar AS, Anuradha CV. Effect of galangin supplementation on oxidative damage and inflammatory changes in fructose-fed rat liver. *Chem Biol Interact* 2011;193:141–8.
- [25] Sivakumar AS, Viswanathan P, Anuradha CV. Dose-dependent effect of galangin on fructose-mediated insulin resistance and oxidative events in rat kidney. *Redox Rep* 2010;15:224–32.
- [26] Huh JE, Junq IT, Choi J, Baek YH, Lee JD, Park DS, et al. The natural flavonoid galangin inhibits osteoclastic bone destruction and osteoclastogenesis by suppressing NF- κ B in collagen-induced arthritis and bone marrow-derived macrophages. *Eur J Pharmacol* 2013;698:57–66.
- [27] Suh KS, Choi EM, Lee YS, Kim YS. Protective effect of albiflorin against oxidative-stress-mediated toxicity in osteoblast-like MC3T3-E1 cells. *Fitoterapia* 2013;89:33–41.
- [28] Feng YL, Tang XL. Effect of glucocorticoid-induced oxidative stress on the expression of Cbfa1. *Chem Biol Interact* 2014;207:26–31.
- [29] Huang Q, Gao B, Wang L, Hu YQ, Lu WG, Yang L, et al. Protective effects of myricitrin against osteoporosis via reducing reactive oxygen species and bone-resorbing cytokines. *Toxicol Appl Pharmacol* 2014;280:550–60.
- [30] Huang Q, Gao B, Jie Q, Wei BY, Fan J, Zhang HY, et al. Ginsenoside-Rb2 displays anti-osteoporosis effects through reducing oxidative damage and bone-resorbing cytokines during osteogenesis. *Bone* 2014;66:306–14.
- [31] Kim JL, Kang SW, Kang MK, Gong JH, Lee ES, Han SJ, et al. Osteoblastogenesis and osteoprotection enhanced by flavonolignan silibinin in osteoblasts and osteoclasts. *J Cell Biochem* 2012;113:247–59.
- [32] Nazrun AS, Norazlina M, Norliza M, Nirwana SI. The anti-inflammatory role of vitamin e in prevention of osteoporosis. *Adv Pharmacol Sci* 2012;2012. Article ID 142702, 7 pages.
- [33] Lin SE, Huang JP, Wu LZ, Wu T, Cui L. Prevention of osteopenia and dyslipidemia in rats after ovariectomy with combined aspirin and low-dose diethylstilbestrol. *Biomed Environ Sci* 2013;26:249–57.
- [34] Cui L, Wu T, Li QN, Lin LS, Liang NC. Preventive effects of ginsenosides on osteopenia of rats induced by ovariectomy. *Acta Pharmacol Sin* 2001;22:428–34.
- [35] Cui L, Wu T, Liu YY, Deng YF, Ai CM, Chen HQ. Tanshinone prevents cancellous bone loss induced by ovariectomy in rats. *Acta Pharmacol Sin* 2004;25:678–84.
- [36] FDA Guidance for industry and reviews 2002: estimating the safe starting dose in clinical trials for therapeutics in adult healthy volunteers 12, <http://www.doc88.com/p-992316940846.html>.
- [37] Huang JH, Huang XH, Chen ZY, Zhens Q, Sun R. Dose conversion among different animals and healthy volunteers in pharmacological study. *Chin J Clin Pharmacol Ther* 2004;9:1069–72.
- [38] Gao SG, Cheng L, Li KH, Liu WH, Xu M, Jiang W, et al. Effect of epimedium pubescens flavonoid on bone mineral status and bone turnover in male rats chronically exposed to cigarette smoke. *BMC Musculoskelet Disord* 2012;13:105–15.
- [39] Yu K, Yang KY, Ren XZ, Chen Y, Liu XH. Amifostine protects bone marrow from benzene-induced haematotoxicity in mice. *Int J Toxicol* 2007;26:315–23.
- [40] Arjmandi BH, Lucas EA, Juma S, Soliman A, Stoecker BJ, Khalil DA, et al. Dried plums prevent ovariectomy-induced bone loss in rats. *JANA* 2001;4:50–6.
- [41] Chang W, Tu C, Chen T, Bikle D, Shoback D. The extracellular calcium-sensing receptor (CaSR) is a critical modulator of skeletal development. *Sci Signal* 2008;1(35):ra1. <http://dx.doi.org/10.1126/scisignal.1159945>.
- [42] Liao C, LIU YY, Wu T, Ai CM, Chen HQ. Osteogenic effects of D(+)- β -3,4-dihydroxyphenyl lactic acid (salvianolic acid A, SAA) on osteoblasts and bone marrow stromal cells of intact and prednisone-treated rats. *Acta Pharmacol Sin* 2009;30:321–32.
- [43] Orsolic N, Goluz E, Dikic D, Lisičić D, Sašilo K, Rodak E, et al. Role of flavonoids on oxidative stress and mineral contents in the retinoic acid-induced bone loss model of rat. *Eur J Nutr* 2014;53:1217–27.
- [44] Polvani S, Tarocchi M, Galli A. PPAR γ and oxidative stress: Con(beta) catenating NRF2 and FOXO. *PPAR Res* 2012;2012. Article ID 641087, 15 pages.
- [45] Manolagas SC. From oestrogen-centric to aging and oxidative stress: a revised perspective of the pathogenesis of osteoporosis. *Endocr Rev* 2010;31:266–300.
- [46] Muthusami S, Ramachandran I, Muthusamy B, Vasudevan G, Prabhu V, Subramaniam V, et al. Ovariectomy induces oxidative stress and impairs bone antioxidant system in adult rats. *Clin Chim Acta* 2005;360:81–6.
- [47] Lee DH, Lim BS, Lee YK, Yang HC. Effects of hydrogen peroxide (H₂O₂) on alkaline phosphatase activity and matrix mineralisation of odontoblast and osteoblast cell lines. *Cell Biol Toxicol* 2006;22:39–46.
- [48] Yang YJ, Su YJ, Wang D, Chen Y, Wu T, Li G. Tanshinol attenuates the deleterious effects of oxidative stress on osteoblastic differentiation via Wnt/FoxO3a signaling. *Oxid Med Cell Longev* 2013;2013. Article ID 351895, 18 pages.
- [49] Awang D. Ginger. *Can Pharm J* 1992;125:309–11.
- [50] Tschirch A. *Handbuch der Pharmakognosie [A handbook of pharmacognosy]*. Leipzig: Verlag CH Tauchnitz; 1923.
- [51] Altman RD, Marcussen KC. Effects of a ginger extract on knee pain in patients with osteoarthritis. *Arthritis Rheuma* 2001;44:2531–8.